Thermokinetic and Structural Shape Memory Effect Characteristics of Novel Quaternary CuAlNiCr HTSMA

Oktay KARADUMAN[1], İskender ÖZKUL[2], Gökhan İSTEK[3], Canan Aksu CANBAY[4*]

[1] Rare Earth Elements Application and Research Center (MUNTEAM), Munzur University, 62000, Tunceli/TURKEY
[2] Department of Mechanical Engineering, Faculty of Engineering, Mersin University, Mersin, TURKEY
[3,4] Physics Department, Faculty of Science, Firat University, Elazig/TURKEY
[*4] caksu@firat.edu.tr

Abstract: CuAlNi shape memory alloys (SMAs) are one of the most prominent Cu-based SMAs mainly due to their shape memory properties at high temperatures. Therefore, they are interested in high temperature SMA applications. Their good thermal stability but brittleness originated from their coarse grain size are their other pros and cons. In this study, the low-cost quaternary CuAlNiCr high-temperature SMA (HTSMA) with a new unprecedented chemical composition including trace amount of chromium element was fabricated by arc melting technique. After arc melting process, traditional homogenization of small alloy samples in the high β-phase temperature region and quenching them in iced-brine water were proceeded. To characterize the shape memory effect property of the alloy, differential calorimetry and microstructural X-ray diffraction (XRD) tests were carried out. The cyclic DSC (differential scanning calorimetry) tests carried out at various heating/cooling rates showed the splendid endothermic and exothermic peaks of reversible martensitic phase transformations in the temperature range between around 150-220 °C, thence the produced alloy is qualified as a high-temperature SMA. Using DSC peak analysis data, the finish and start temperatures of every martensitic phase transition, hysteresis gap, plus some other important thermodynamic parameters' values were also determined. Among them, the high enthalpy change amounts occurred during the transformations implied the good shape memory effect feature of the alloy. A DTA (differential thermal calorimetry) test taken at only one heating/cooling rate revealed both the reversible martensitic transformation peaks and the other phase transition peaks at higher temperatures. The consecutive phase transition step peaks of $\beta'1 \rightarrow B1(L2_1) \rightarrow B2 \rightarrow A2$ on the heating-part of the DTA thermogram curve of the alloy were observed as similar to those seen in the other Cu-based shape memory alloys. Furthermore, at room temperature, the presence and types of the martensite phases formed in the alloy were revealed by the XRD pattern of the alloy obtained by using CuKα radiation. The results showed that the novel CuAlNiCr high-temperature SMA can be useful in the high-temperature SMA applications.

Key words: High-temperature shape memory alloy, CuAlNiCr, martensitic transformation, DSC, DTA.

Termodinamik ve Yapısal Şekil Hafıza Etkisinin Dörtlü CuAlNiCr YSŞHA Karakteristikleri

Öz: CuAlNi şekil hafızalı alaşımlar (ŞHA'lar), esas olarak yüksek sıcaklıklardaki şekil hafızalı özelliklerinden dolayı en öne çıkan Cu-bazlı ŞHA'lardandır. Bu ŞHA'lara bu nedenle yüksek sıcaklık ŞHA uygulamalarında ilgi duyulmaktadır. İyi termal kararlılıkları ancak iri tane boyutlarından kaynaklanan kırılganlıkları diğer artıları ve eksileridir. Bu çalışmada, eser miktarda krom elementi içeren benzersiz bir kimyasal bileşime sahip dörtlü CuAlNiCr yüksek sıcaklık ŞHA (YSŞHA), ark eritme tekniği ile üretildi. Ark eritme işleminden sonra, küçük alaşım numunelerinin yüksek β fazı sıcaklık bölgesinde geleneksel homojenleştirilip tuzlu buzlu suda hızlıca soğutuldu. Alaşımın şekil hafıza etkisi özelliğini karakterize etmek için diferansiyel kalorimetri ve mikroyapısal X-ışını kırınımı (XRD) testleri gerçekleştirildi. Farklı ısıtma/soğutma hızlarında gerçekleştirilen diferansiyel taramalı kalorimetri (DSC) testleri, yaklaşık 150-220 °C arasındaki sıcaklık aralığında tersinir martensitik faz dönüşümlerinin olağanüstü ekzotermik ve endotermik piklerini gösterdi; bundan dolayı üretilen alaşım bir yüksek sıcaklık ŞHA olarak sınıflandırıldı. DSC pik analizi verileri kullanılarak her bir martensitik faz dönüşümünün başlangıç ve bitiş sıcaklıkları, histeresiz aralığı ve diğer bazı önemli termodinamik parametreleri belirlendi. Bunlar arasında, dönüşümler sırasında meydana gelen yüksek entalpi değişim miktarları, alaşımın iyi şekil hafıza etkisi özelliğine sahip olduğuna işaret etmiştir. Tek bir ısıtma/soğutma hızında daha yüksek sıcaklıklara kadar çıkılarak yapılan diferansiyel termal kalorimetri (DTA) testi, hem tersinir martensitik dönüşüm piklerini yine ve hem de diğer faz geçiş piklerinin oluştuğunu gösterdi. Alaşımın DTA eğrisinin ısınma kısmında $\beta'1 \rightarrow B1(L2_1) \rightarrow B2 \rightarrow A2$ ardışık faz geçiş adımı pikleri diğer Cu bazlı şekil hafızalı alaşımlarda görülenlere benzer şekilde gözlendi. Ayrıca oda sıcaklığında alaşımda oluşan martensit fazların varlığı, alaşımın CuKα radyasyonu kullanılarak elde edilen XRD deseni ile ortaya çıkarılmıştır. Sonuçlar, yeni CuAlNiCr yüksek sıcaklık ŞHA'sının yüksek sıcaklık ŞHA uygulamalarında faydalı olabileceğini gösterdi.

Anahtar kelimeler: Yüksek sıcaklık şekil hafızalı alaşım, CuAlNiCr, martensitik dönüşüm, DSC, DTA.

[*] Corresponding Author: caksu@firat.edu.tr. ORCID Numbers of Authors: [1] 0000-0002-6947-7590, [2] 0000-0003-4255-0564, [4] 0000-0002-5151-4576

1. Introduction

As it is renowned, shape memory alloys (SMAs) [1,2], which are the second most commercial smart material group after piezoelectrics, have been extensively studied due to their unique and magic-like shape memory effect (SME), superelasticity and excellent damping properties. These properties made these materials very attractive and useful in many industrial and technological application fields such as actuator, automotive, medical, aerospace, robotics, construction, energy harvesting/converting, micro and nano electromechanic systems (M/NEMSs), textile, etc. [1–8].

In most of applications nickel-titanium (NiTi) SMAs [9,10] are used due to their superior shape memory and superelastic properties. Although NiTi SMAs have already been commercially used in numerous applications such as medical, aerospace or automotive [9,11–14], thus having great importance, the processability or machinability of these SMAs is relatively hard arising from their high ductility and deformation hardening, high chemical reactivity, low thermal conductivity and elastic modulus which results in poor surface finish and poor tool life [15,16]. But nearly ten times cheaper copper-based SMAs are thought as the nearest alternative to NiTi SMAs. The mechanism of shape memory effect property of SMAs depends on a solid-to-solid phase transition known as martensitic transformation. Martensitic transformations occur reversibly, atomically non-diffusional and isostatical between two different solid phases of SMAs called as the product phase or martensite (low-temperature phase) and the parent or austenite (high-temperature) phase [1]. A martensitic transformation can be occur when SMAs are exposed to external forces such as heat or ellectric/magnetic fields, the internal crystal lattice stresses occur by the external forces and these stesses impell the unit cell of a martensitic phase to change into the other unite cell of other martensitic phase. The total changes of all unit cells results a macro size shape change in SMAs that we can see. For example, when the temperature goes down to a critical level by cooling a NiTi SMA [9,17], a cubic lattice structure of austenite phase can transform into a martensite phase with a monoclinic lattice structure. This type of transformation from austenite to martensite is called as forward martensitic transformation. If temperature increase up again, at this time a reverse martensitic transformation occurs from martensite to austenite. The finish and start temperatures of reverse transformation (to parent phase) and forward (to martensite) transformation reactions, from the highest to the lowest, are ranked as $A_f > A_s > M_s > M_f$. Austenite phase becomes disordered after a critical M_d ($>A_f$) temperature, and between A_f and M_d temperatures SMAs can exhibit superelasticity (pseudoelasticity) [18,19]. If SMAs are made deformed plastically by a mechanical force or stress (load) when they are in martensite phase, then if the load is removed away and they are exposed to heat, a reverse transformation take place and accordingly they return back to their pre-deformed original shape. But when SMAs are cooled down to the martensite temperature region they will not take the deformed shape back again and this is known as one-way shape memory effect (OWSME), and if some extra training treatments applied they can also show two-way shape memory effect (TWSME) [19].

NiTi, Cu-based (Cu-rich) and Fe-based (Fe-rich) SMA bases are three primary SMAs families. Among these, practically and industrially NiTi SMAs are the most preffered ones due to their superlative SE and SME features. But NiTi ones are much more expensive and arduously processable when compared to Cu-based ones showing better SE and SME than those of iron-based SMAs. For this reason, Cu-based SMAs are deemed as the nearest alternative to NiTi ones [20]. They are regarded as an alternative to be used in high-temperature operations and to other commercial SMAs because of their lesser production costs, too [20]. In spite of that Cu-based SMAs have been considerably investigated, they have still many issues to be overcome. Polycrystalline Cu-based SMAs exhibit some drawbacks such as their brittleness, and thermal instability or instability of martensite and austenite phases that affects transformation temperatures, hysteresis, strain recovery i.e. the shape memory properties. These problems stems mainly from the coarse grains, defects or types of martensite and are also highly dependent on the material production/processing history and the composition of these alloys [20]. A common way used to solve these problems is adding some grain-refiner elements like Be, Ni, Ti, Mg, Fe, Zn, Mn, Co, etc. in these SMAs [20–28]. The shape memory properties of the SMAs are extremely sensitive to their alloying compositions.

The shape memory effect mechanism of Cu-based SMAs depending on a martensitic transformation from usually a cubic β-phase (DO_3 or $L2_1$) which is high symmetry austenite (A) phase to a low symmetry martensite (M) phase. Martensite phase in Cu-based SMAs can mostly form in monoclinic (β'), orthorhombic (γ') or β'' (a mix of β'+γ') forms depending on the alloy composition and also on the stress level of these alloys [5,20,27]. The low-temperature martensitic phases that can be found in these alloys are: α1'(3R) observed for low Al contents, β1'(18R) for intermediate (9-14 wt.%) Al contents, and γ1'(2H) that is predominant in alloys with high Al contents [20,29].

The customary CuAlNi and CuZnAl SMAs and CuAlMn, CuAlFeMn and CuAlBe SMAs are the most salient Cu-based SMAs [1,20,24,30]. Cu-based SMAs, especially CuAlNi ones, are more capable than NiTi SMAs in terms of operating at high temperatures [5,31–44].

The effect of Cr element on CuAlNi SMAs has not been adequately studied before, except only three studies [45–47] on CuAlNiCr alloys, two of them with low martensitic transformation temperatures, and different alloying

compositions have been found in the literature. Also, there were some other works but they are not about shape memory aspects. The effects of adding chromium on CuAlNi , therefore, still have not understand well.

The addition of chromium (Cr) to copper-aluminum (Cu-Al) SMAs can significantly influence their microstructure, phase stability, and transformation temperatures [48–50] , thereby enhancing their shape memory properties and expanding their potential applications. Notably, the addition of Cr to Cu-Al SMAs has been reported to enhance the thermal and compositional stability of the alloy, forming stable precipitates.

In this study, the quaternary CuAlNiCr with unprecedented 72.56Cu-22.34Al-4.34Ni-0.77Cr (at.%) composition was manufactured in an arc melter. The characteristic shape memory effect parameters were revealed by differential calorimetric DSC and DTA measurements and based analyses and calculations, and by structural XRD test.

2. Experimental

The CuAlNiCr high-temperature SMA was manufactured by melting the pellets obtained by pressing powder mixture of highly pure (%99.9) metal powders of Cu, Al, Ni, and Cr in a vacuum arc melter. After arc melting, the alloy obtained as-casted ingot was sliced as proper test samples. Then these test samples were homogenized at 900 ºC for 1 h and immediately immersed (quenched) in iced-brine water (to form martensitic structure in the alloy by this rapid cooling). The DSC tests were performed out via using a Shimadzu-60A label DSC equipment at varied heating/cooling rates of 10, 15, 20 and 25 °C/min under inert (argon) gas with a constant flow rate of 100 ml/min for revealing thermally induced shape memory behavior. By using a Shimadzu DTG-60AH instrument the DTA test was performed out at a single 25 °C/min of heating/cooling rate between room temperature and high beta-phase temperature region under same inert gas condition to observe behavior of the alloy at high temperatures. The XRD pattern of the alloy was obtained in room conditions via using a Rigaku Miniflex 600 model X-ray diffractometer (by using CuKα wavelenght rays) for revealing the formed martensite phases in the alloy matrix. The EDS analysis was made to determine the alloying composition of the CuAlNiCr alloy by using a SEM-Hitachi SU3500 instrument at room temperature.

3. Results and Discussion

The detected 72.56Cu-22.34Al-4.34Ni-0.77Cr (at.%) alloying composition of the CuAlNiCr HTSMA obtained by the EDS test result is given in Figure 1, and in Table 1. Average electron concentration per atom (e/a) ratio of the CuAlNiCr HTSMA was calculated as 1.49 by substituting the (at.%)-fractions of every metal element of the detected alloy composition in the formula [27] expressed as $e/a = \Sigma f_i.v_i$, where f represents the (at.%)-fractions of the alloying elements and v refers to the corresponding valency (numbers) of these elements. Thus, the e/a ratio of the CuAlNiCr alloy was found as 1.49. This e/a parameter of the produced CuAlNiCr alloy is fall in between the e/a ratio range of 1.45-1.51 which range is regarded as a theoretical condition for copper-based alloys to exhibit most probably a shape memory effect [1,27]. Also, in this e/a ratio range Cu-based SMAs are expected to have two different martensite forms (β1′ and γ1′) together.
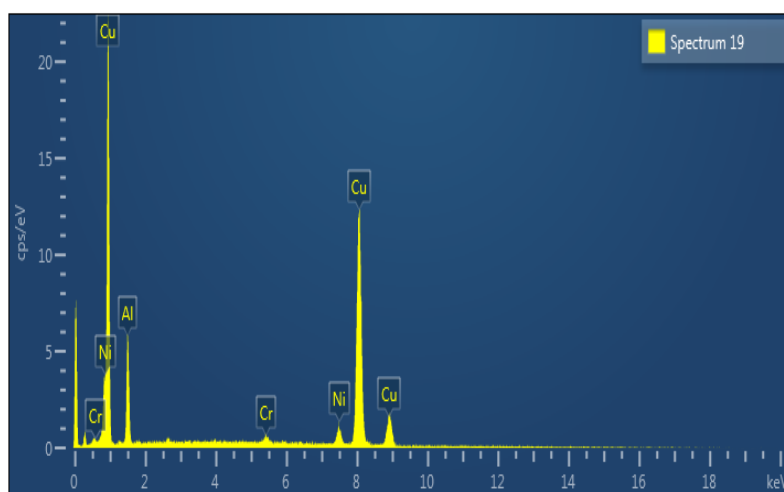

Figure 1. The EDS test result of the CuAlNiCr HTSMA.

Table 1. The EDS alloy composition of the CuAlNiCr HTSMA.

	Cu	Al	Ni	Cr
Atomic percentage (at.%)	72.56	22.34	4.34	0.77

The multi-curves DSC results each at different heating/cooling heating rate are given in Figure 2 show the formation of down endothermic and up exothermic solid-to-solid reaction peaks indicating the reversible martensitic phase transformations of the CuAlNiCr HTSMA. The cycling DSC heating/cooling curves taken at different 10 - 25 °C/min of rates show the highly stable reverse (martensite to austenite; M→A) transformation on heating fragments of these thermograms and the forward austenite to martensite (A→M) transitions on cooling fragments of these curves [18,27,51] due to very slightly changes of peak positions and no any peak splitting observed as occurence of secondary phase transitons [52] on or near these peaks even after several time of DSC runnings at different heating/cooling rates.
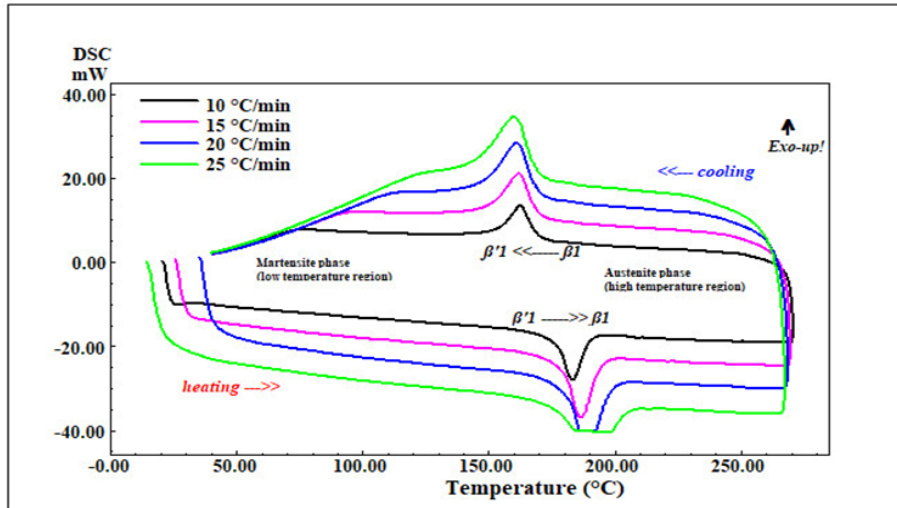

Figure 2. The multiple DSC curves of the CuAlNiCr HTSMA obtained at different heating/cooling heating rates.

The characteristic martensitic transformation temperatures and other thermodynamic parameter values of the CuAlNiCr HTSMA obtained from the DSC peak analyses data and calculations based on were given in Table 2. In this table, the thermal equilibrium temperature (T_0) parameter values, at where there is zero gap between the Gibbs (chemical) free energies of austenite and martensite phases, were determined by $T_0=(A_f+M_s)/2$ formula [27]. And, the entropy change (ΔS) happened with M→A reactions were calculated by using the enthalpy ΔH change values in $\Delta S_{M\rightarrow A}=\Delta H_{M\rightarrow A}/T_0$ formula [27]. The high martensitic transformation temperatures of the produced CuAlNiCr alloy was found ranging in between 146.29 °C (the minimum M_f) and 204.45 °C (the maximum A_f) temperatures range which range is found higher than the range of 37.53 °C and 113.22 °C [45], -44.66 °C and -6.09 °C [46] reported in previous works. So, the transformation temperatures range determined in this work being much higher than those reported in previous works [45,46] is found as unique and the only high-temperatures range and thus the only high-temperature CuAlNiCr shape memory alloy, too.

Table 2. The characteristic temperatures of martensitic transformation and thermodynamic parameters of the fabricated CuAlNiCr HTSMA.

Heating/cooling rate (°C/min)	A_s (°C)	A_f (°C)	A_{max} (°C)	M_s (°C)	M_f (°C)	A_s-M_f (°C)	T_0 (°C)	$\Delta H_{M \to A}$ (J/g)	$\Delta S_{M \to A}$ (J/g°C)
10	177.12	189.57	183.39	169.58	153.93	23.19	179.58	13.54	0.0754
15	179.38	194.00	186.54	169.63	150.89	28.49	181.82	13.57	0.0746
20	180.52	198.14	191.31	169.46	148.02	32.50	183.80	12.06	0.0656
25	174.42	204.45	197.57	168.93	146.29	28.13	186.69	8.97	0.0480
Avg.	177.86	196.54	189.70	169.40	149.78	28.08	182.97	12.04	0.0659

The transformation temperatures and thermodynamic parameters of CuAlNiCr HTSMA changing with heating/cooling rate were also displayed as plots given in Figure 3-a and -b. By the increase of heating/cooling rate, while A_f and T_0 temperatures are seen increased, M_f temperature is seen decreased, and the enthalpy and entropy change values of reverse transformation are both seen decreased. The faster heating, the lower volume of martensite allowed to transform to austenite. Because, for a fully transformation enough time keeping at same isostatic temperature (more like a small temperature interval) is needed, since martensitic transformations occur isostatically. When the heating rate is high the temperature goes up so rapidly leaving some of martensites un-transformed behind. Some times, at much higher rates, a temperature lag (lag of A_f) occurs as a sign of late transformation of the rest un-transformed martensites [17].
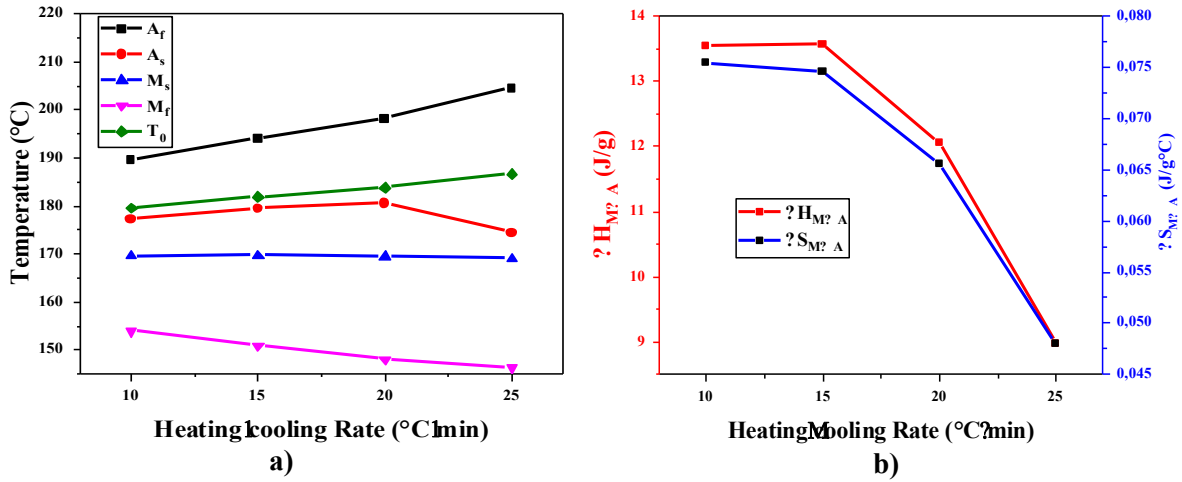
Figure 3. The plots showing a) the transformation temperatures and b) kinetic parameters of CuAlNiCr HTSMA changing with heating/cooling rate.

The kinetic activation energy (E_a) is a determining parameter in formation of martensitic transformation reaction and crystallization of the alloy. Here, for the activation energy of the CuAlNiCr HTSMA the below-given Kissinger formula in eq. (1) [27,53] was used;

$$\frac{d\left[ln\left(\frac{\phi}{T_m^2}\right)\right]}{d\left(\frac{1}{T_m}\right)} = -\frac{E_a}{R} \tag{1}$$

where; T_m is maximum austenite formation (M→A) peak temperature (A_{max}), ϕ is heating/cooling rate, R is the universal gas constant (R=8.314 J/mol.K). The plot of activation energy change of the reverse transformation of the CuAlNiCr HTSMA is given in Figure 4. The lineer fitting-slope of this plot represents the left term of the Eq.1. By using slope value instead of the left term in Eq.1, the E_a activation energy value of the reverse martensitic phase transition of the produced CuAlNiCr HTSMA was computed as 102.55 kJ/mol.
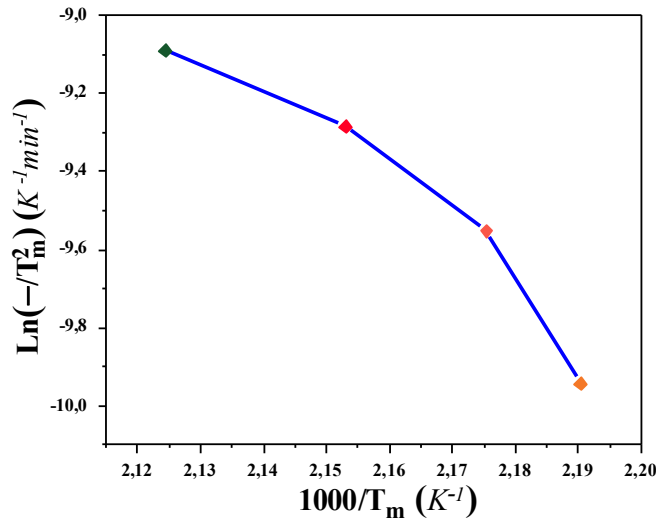
Figure 4. The activation energy change plot of the reverse martensitic transformation of the CuAlNiCr HTSMA.

The cyclic DTA curve taken at single 25 °C/min of heating/cooling rate given in Figure 5 shows the reverse and forward martensitic transformation peaks again and also the other thermally induced phase transitions reactions in the CuAlNiCr HTSMA at high temperatures. A phase transition chain observed on heating as follows: martensite (β1′) →austenite (β1, L2₁) → B2 (metastable cubic) → precipitating → eutectoid recomposition → B2 (ordered cubic) →A2 (disordered cubic) [1,27,51,54,55] and this phase transitions chain is seen common in Cu-based SMAs. The eutectoid point (this peak is seen formed at 500 °C circa on heating part, and vice versa on cooling part) indicates the dissolution of precipitations (that form before this peak) into β (or B2) phase. Here, the forward martensitic transformation (β1→β1′) peak is seen on cooling the CuAlNiCr alloy become smaller as compared with the sharp and large reverse one (β1′ →β1) seen on heating. The reason for this is that the alloy's composition or structure might have been some changed in some local domains when passing through the high temperature region of precipitating and eutectoid region. Precipitations occur by diffusion of atoms at high temperatures, and they disarrange some of martensitic structure, i.e. lead to a reduction of some shape memory capacity understood from the shrinking of transformation peak. By giving an extra heating of the CuAlNiCr HTSMA up to β-phase temperature region above its eutectoid point (the peak seen formed at 500 °C circa on heating part) and then by rapidly quenching the alloy from that high temperature can be done to bring the forward transformation peak (shape memory capacity) back to its normal size again.
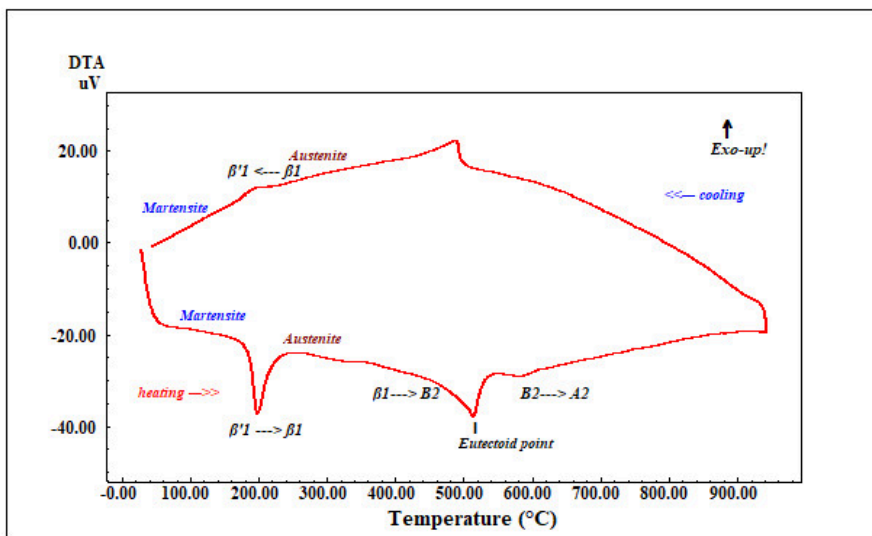

Figure 5. The DTA termogram of the CuAlNiCr HTSMA.

The XRD pattern of the CuAlNiCr HTSMA is given in Figure 6 and it shows the formed martensitic phases in the alloy at room temperature. Here, the main observed peak is β1′(122) martensite peak, and the others are also some β1′ and some γ1′ type martensite peaks [25,27,28,38,56–59]. The XRD pattern of the CuAlNiCr HTSMA shows the co-existence of monoclinic β1′ (18R) and orthorhombic γ1′ (2H) type martensite phases just as above-predicted over the e/a ratio of the alloy.
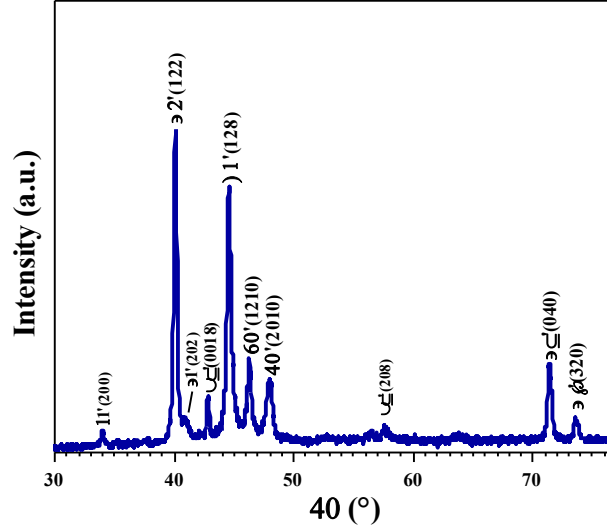

Figure 6. The XRD pattern of the CuAlNiCr HTSMA.

The mean size of the ordered (crystalline) domains, i.e. the Debye-Scherrer crystallite size (*D*) of the alloy was also calculated by using Debye-Scherrer formula [27] as below in (2);

$$D = \frac{0.9\lambda}{B_{\frac{1}{2}}\cos\theta} \tag{2}$$

where; λ refers to the used wavelength (CuKα radiation, λ= 0.15406 nm) of X-ray diffracted from the surface of the alloy in the XRD test, $B_{1/2}$ stands for the full width at half maximum (FWHM) value of the highest intensity peak, and θ represents the Bragg angle of the diffraction. The crystallite size *D* values were determined as 29.69 nm by using the FWHM value of the highest β1′ (122) peak at the 2θ angle of 40.14°.

4. Conclusions

The quaternary CuAlNiCr HTSMA was manufactured succesfully by arc melting technique and the shape memory effect characterization of the alloy was made by differential calorimetry (DSC, DTA) and structural (XRD, EDS) measurements.

The DSC results showed the powerful and stable reversible martensitic transformation peaks at the temperatures above 100 °C approximately between 150 °C and 200 °C, and also the DTA curve on heating showed the multi-step phase transitions chain of β1′(or β1′+γ1′) → β1(L2₁) → B2 → A2 which is common to the Cu-based shape memory alloys. Heating up above eutectoid point can reduce the enthalpy change of martensitic transformation and shape memory effect capacity of the alloy due to some local compositional changes might have been originated from some residual precipitations and intermetallic phases emerging during the heating and some remaining during cooling back. In this case, an additional heating the alloy up to its high beta-phase temperature region and quenching will probably be the convenient remedy to entirely re-build the martensitic structure of shape memory mechanism in the alloy again.

The XRD result showed the co-existence of β1′and γ1′ type martensites which constitutes the base crystallographic mechanism for the shape memory effect property of the CuAlNiCr HTSMA.

The obtained results showed that the new composition CuAlNiCr HTSMA can be useful in various HTSMA related applications. The results obtained in this study on CuAlNiCr HTSMA will help in research and development on Cu-based SMAs, CuAlNi SMAs and Cr incorporated CuAl-based SMAs which are demanded for their low cost and some relatively more practical fabrication ease than NiTi SMAs, also brings new literature

information that will be used by the researchers in their perspectives and in future works. Moreover, the next work can be done on the ternary CuAlCr alloy with more amount of Cr addition to see the effect of Cr on CuAl-base system and its shape memory and microstructure properties.

Acknowledgments

References

[1]   Otsuka K, Wayman CM. Shape memory materials. Cambridge University Press; 1999.
[2]   Fernandes DJ, Peres R V., Mendes AM, Elias CN. Understanding the Shape-Memory Alloys Used in Orthodontics. ISRN Dent 2011;2011:1–6. https://doi.org/10.5402/2011/132408.
[3]   Muthukumarana S, Messerschmidt MA. Clothtiles: A prototyping platform to fabricate customized actuators on clothing using 3d printing and shape-memory alloys. Conference on Human Factors in Computing Systems - Proceedings 2021. https://doi.org/10.1145/3411764.3445613.
[4]   Concilio A, Antonucci V, Auricchio F, Lecce L, Sacco E (Eds.). Shape Memory Alloy Engineering. 2nd ed. Elsevier; 2 021. https://doi.org/10.1016/C2018-0-02430-5.
[5]   Ma J, Karaman I, Noebe RD. High temperature shape memory alloys. International Materials Reviews 2010;55:257–315. https://doi.org/10.1179/095066010X12646898728363.
[6]   Rao A, Srinivasa AR, Reddy JN. Introduction to shape memory alloys. SpringerBriefs in Applied Sciences and Technology 2015:1–31. https://doi.org/10.1007/978-3-319-03188-0_1.
[7]   Hartl DJ, Lagoudas DC. Aerospace applications of shape memory alloys. Proceedings of the Institution of Mechanical Engineers, Part G: Journal of Aerospace Engineering 2007;221:535–52. https://doi.org/10.1243/09544100JAERO211.
[8]   Fu YQ, Luo JK, Flewitt AJ, Huang WM, Zhang S, Du HJ, et al. Thin film shape memory alloys and microactuators. Int J Computational Materials Science and Surface Engineering 2009;2:208–26. https://doi.org/10.1504/IJCMSSE.2009.027483.
[9]   Mwangi JW, Nguyen LT, Bui VD, Berger T, Zeidler H, Schubert A. Nitinol manufacturing and micromachining: A review of processes and their suitability in processing medical-grade nitinol. J Manuf Process 2019;38:355–69. https://doi.org/https://doi.org/10.1016/j.jmapro.2019.01.003.
[10]   Kauffman GB. The Story of Nitinol: The Serendipitous Discovery of the Memory Metal and Its Applications. The Chemical Educator 1997;2:1–21. https://doi.org/10.1007/s00897970111a.
[11]   Kim WC, Lim KR, Kim WT, Park ES, Kim DH. Recent advances in multicomponent NiTi-based shape memory alloy using metallic glass as a precursor. Prog Mater Sci 2021;118. https://doi.org/10.1016/j.pmatsci.2020.100756.
[12]   Hite N, Sharar DJ, Trehern W, Umale T, Atli KC, Wilson AA, et al. NiTiHf shape memory alloys as phase change thermal storage materials. Acta Mater 2021;218. https://doi.org/10.1016/j.actamat.2021.117175.
[13]   Riccio A, Sellitto A, Ameduri S, Concilio A, Arena M. Shape memory alloys (SMA) for automotive applications and challenges. Shape Memory Alloy Engineering: For Aerospace, Structural, and Biomedical Applications 2021:785–808. https://doi.org/10.1016/B978-0-12-819264-1.00024-8.
[14]   Costanza G, Tata ME. Shape Memory Alloys for Aerospace, Recent Developments, and New Applications: A Short Review. Materials 2020;13. https://doi.org/10.3390/ma13081856.
[15]   Altas E, Gokkaya H, Karatas MA, Ozkan D. Analysis of surface roughness and flank wear using the taguchi method in milling of niti shape memory alloy with uncoated tools. Coatings 2020;10:1–17. https://doi.org/10.3390/coatings10121259.
[16]   Altas E, Altin Karatas M, Gokkaya H, Akinay Y. Surface Integrity of NiTi Shape Memory Alloy in Milling with Cryogenic Heat Treated Cutting Tools under Different Cutting Conditions. J Mater Eng Perform 2021;30:9426–39. https://doi.org/10.1007/s11665-021-06095-3.
[17]   Canbay CA, Karaduman O, Özkul İ. Lagging temperature problem in DTA/DSC measurement on investigation of NiTi SMA. Journal of Materials Science: Materials in Electronics 2020;31:13284–91. https://doi.org/10.1007/s10854-020-03881-y.
[18]   Babacan N, Pauly S, Gustmann T. Laser powder bed fusion of a superelastic Cu-Al-Mn shape memory alloy. Mater Des 2021;203. https://doi.org/10.1016/j.matdes.2021.109625.
[19]   Mohd Jani J, Leary M, Subic A, Gibson MA. A review of shape memory alloy research, applications and opportunities. Mater Des 2014;56:1078–113. https://doi.org/10.1016/j.matdes.2013.11.084.
[20]   Mazzer EM, Da Silva MR, Gargarella P. Revisiting Cu-based shape memory alloys: Recent developments and new perspectives. J Mater Res 2022;37:162–82. https://doi.org/10.1557/s43578-021-00444-7.
[21]   Sugimoto K, Kamei K, Matsumoto H, Komatsu S, Akamatsu K, Sugimoto T. Grain-refinement and the related phenomena in quaternary Cu-Al-Ni-Ti shape memory alloys. Le Journal de Physique Colloques 1982;43:C4-761-C4-766. https://doi.org/10.1051/jphyscol:19824124.

[22] Yang J, Wang QZ, Yin FX, Cui CX, Ji PG, Li B. Effects of grain refinement on the structure and properties of a CuAlMn shape memory alloy. Materials Science and Engineering A 2016;664:215–20. https://doi.org/10.1016/j.msea.2016.04.009.

[23] Sutou Y, Omori T, Yamauchi K, Ono N, Kainuma R, Ishida K. Effect of grain size and texture on pseudoelasticity in Cu-Al-Mn-based shape memory wire. Acta Mater 2005;53:4121–33. https://doi.org/10.1016/j.actamat.2005.05.013.

[24] Dasgupta R. A look into Cu-based shape memory alloys: Present scenario and future prospects. J Mater Res 2014;29:1681–98. https://doi.org/10.1557/jmr.2014.189.

[25] Najib ASM, Saud SN, Hamzah E. Corrosion Behavior of Cu–Al–Ni–xCo Shape Memory Alloys Coupled with Low-Carbon Steel for Civil Engineering Applications. J Bio Tribocorros 2019;5. https://doi.org/10.1007/s40735-019-0242-8.

[26] Canbay CA, Karaduman O, Özkul İ. Investigation of varied quenching media effects on the thermodynamical and structural features of a thermally aged CuAlFeMn HTSMA. Physica B Condens Matter 2019;557:117–25. https://doi.org/10.1016/j.physb.2019.01.011.

[27] Canbay CA, Karaduman O, Ünlü N, Baiz SA, Özkul İ. Heat treatment and quenching media effects on the thermodynamical, thermoelastical and structural characteristics of a new Cu-based quaternary shape memory alloy. Compos B Eng 2019;174:106940. https://doi.org/10.1016/j.compositesb.2019.106940.

[28] Saud SN, Hamzah E, Abubakar T, Zamri M, Tanemura M. Influence of Ti additions on the martensitic phase transformation and mechanical properties of Cu-Al-Ni shape memory alloys. J Therm Anal Calorim 2014;118:111–22. https://doi.org/10.1007/s10973-014-3953-6.

[29] Svirid AE, Kuranova NN, Lukyanov A V., Makarov V V., Nikolayeva N V., Pushin VG, et al. Influence of Thermomechanical Treatment on Structural-Phase Transformations and Mechanical Properties of the Cu–Al–Ni Shape-Memory Alloys. Russian Physics Journal 2019;61:1681–6. https://doi.org/10.1007/s11182-018-1587-z.

[30] Canbay CA, Karaduman O, Ünlü N, Özkul I. Study on Basic Characteristics of CuAlBe Shape Memory Alloy. Brazilian Journal of Physics 2021;51:13–8. https://doi.org/10.1007/s13538-020-00823-1.

[31] Firstov GS, Van Humbeeck J, Koval YN. High-temperature shape memory alloys. Materials Science and Engineering: A 2004;378:2–10. https://doi.org/10.1016/j.msea.2003.10.324.

[32] Motemani Y, Buenconsejo PJS, Ludwig A. Recent Developments in High-Temperature Shape Memory Thin Films. Shape Memory and Superelasticity 2015;1. https://doi.org/10.1007/s40830-015-0041-0.

[33] Zhang X, Liu Q. Cu-Al-Ni-V high-temperature shape memory alloys. Intermetallics (Barking) 2018;92:108–12. https://doi.org/10.1016/j.intermet.2017.10.001.

[34] Zhang X, Liu Q. Cu-Al-Ni-V high-temperature shape memory alloys. Intermetallics (Barking) 2018;92. https://doi.org/10.1016/j.intermet.2017.10.001.

[35] Yang S, Su Y, Wang C, Liu X. Microstructure and properties of Cu-Al-Fe high-temperature shape memory alloys. Mater Sci Eng B Solid State Mater Adv Technol 2014;185:67–73. https://doi.org/10.1016/j.mseb.2014.02.001.

[36] López-Ferreño I, Gómez-Cortés JF, Breczewski T, Ruiz-Larrea I, Nó ML, San Juan JM. High-temperature shape memory alloys based on the Cu-Al-Ni system: Design and thermomechanical characterization. Journal of Materials Research and Technology 2020;9:9972–84. https://doi.org/10.1016/j.jmrt.2020.07.002.

[37] Van Humbeeck J. Shape memory alloys with high transformation temperatures. Mater Res Bull 2012;47:2966–8. https://doi.org/10.1016/j.materresbull.2012.04.118.

[38] Zhang X, Liu QS. Influence of alloying element addition on Cu-Al-Ni high-temperature shape memory alloy without second phase formation. Acta Metallurgica Sinica (English Letters) 2016;29:884–8. https://doi.org/10.1007/s40195-016-0467-1.

[39] Guilemany JM, Fernández J, Franch R, Benedetti A V., Adorno AT. A New Cu-Based SMA with Extremely High Martensitic Transformation Temperatures. Le Journal de Physique IV 1995;05:C2-361-C2-365. https://doi.org/10.1051/jp4:1995255.

[40] Cheniti H, Bouabdallah M, Patoor E. High temperature decomposition of the β1 phase in a Cu–Al–Ni shape memory alloy. J Alloys Compd 2009;476:420–4. https://doi.org/10.1016/J.JALLCOM.2008.09.003.

[41] Karaduman O, Özkul I, Altın S, Altın E, Bağlayan, Canbay CA. New Cu-Al based quaternary and quinary high temperature shape memory alloy composition systems. AIP Conf Proc, vol. 2042, American Institute of Physics Inc.; 2018. https://doi.org/10.1063/1.5078902.

[42] Wang CP, Su Y, Yang SY, Shi Z, Liu XJ. A new type of Cu-Al-Ta shape memory alloy with high martensitic transformation temperature. Smart Mater Struct 2014;23. https://doi.org/10.1088/0964-1726/23/2/025018.

[43] Karaduman O, Özkul İ, Canbay CA. Shape memory effect characterization of a ternary CuAlNi high temperature SMA ribbons produced by melt spinning method. Advanced Engineering Science 2021;1:26–33.

[44] Canbay CA, Karaduman O, Ünlü N, Özkul İ, Çiçek MA. Energetic Behavior Study in Phase Transformations of High Temperature Cu–Al–X (X: Mn, Te, Sn, Hf) Shape Memory Alloys. Transactions of the Indian Institute of Metals 2021. https://doi.org/10.1007/s12666-021-02241-6.

[45] Zare M, Ketabchi M. Effect of chromium element on transformation, mechanical and corrosion behavior of thermomechanically induced Cu–Al–Ni shape-memory alloys. J Therm Anal Calorim 2017;127:2113–23. https://doi.org/10.1007/s10973-016-5839-2.

[46] Teixeira CA, Coelho RE, Lima PC, Nascimento CS, Mendonça ES, Murilo S, et al. THE EFFECT OF CHROMIUM ON MICROSTRUCTURE OF CUALNI SHAPE MEMORY ALLOY. 24th International Conference on Metallurgy and Materials, Brno, Czech Republic, EU , 2015.

[47] Koo H-S, Chen H, Chen F-H. Microstructural Characteristics and Shape Memory Effect of Rapidly Quenched Cu-Al-Ni-Cr Alloy. MRS Proceedings 1991;246:201. https://doi.org/10.1557/PROC-246-201.

[48] IIJIMA M, ENDO K, OHNO H, MIZOGUCHI I. Effect of Cr and Cu Addition on Corrosion Behavior of Ni-Ti Alloys. Dent Mater J 1998;17:31–40. https://doi.org/10.4012/dmj.17.31.

[49] Amer SM, Glavatskikh M V., Barkov RYu, Loginova IS, Pozdniakov A V. Effect of Cr on the Microstructure and Mechanical Properties of the Al-Cu-Y-Zr Alloy. Metals (Basel) 2023;13:349. https://doi.org/10.3390/met13020349.

[50] da M. Candido GV, de A. Melo TA, De Albuquerque VHC, Gomes RM, de Lima SJG, Tavares JMRS. Characterization of a CuAlBe Alloy with Different Cr Contents. J Mater Eng Perform 2012;21:2398–406. https://doi.org/10.1007/s11665-012-0159-6.

[51] Canbay CA, Karaduman O. The photo response properties of shape memory alloy thin film based photodiode. J Mol Struct 2021;1235:130263. https://doi.org/10.1016/J.MOLSTRUC.2021.130263.

[52] Pinto RDA, Silva RAG. Mirrored symbols, opposite effects: Impact of Ga and Ag additions on the martensite decomposition of the Cu81Al19 alloy. Mater Today Commun 2023;37:107280. https://doi.org/10.1016/j.mtcomm.2023.107280.

[53] Kissinger HE. Reaction Kinetics in Differential Thermal Analysis. Anal Chem 1957;29:1702–6. https://doi.org/10.1021/ac60131a045.

[54] Prado MO, Decorte PM, Lovey F. Martensitic transformation in Cu-Mn-Al alloys. Scripta Metallurgica et Materialia 1995;33. https://doi.org/10.1016/0956-716X(95)00292-4.

[55] Chentouf SM, Bouabdallah M, Gachon JC, Patoor E, Sari A. Microstructural and thermodynamic study of hypoeutectoidal Cu-Al-Ni shape memory alloys. J Alloys Compd 2009;470:507–14. https://doi.org/10.1016/j.jallcom.2008.03.009.

[56] Saud SN, Hamzah E, Abubakar T, Bakhsheshi-Rad HR. Microstructure and corrosion behaviour of Cu-Al-Ni shape memory alloys with Ag nanoparticles. Materials and Corrosion 2015;66:527–34. https://doi.org/10.1002/maco.201407658.

[57] Chentouf SM, Bouabdallah M, Gachon J-C, Patoor E, Sari A. Microstructural and thermodynamic study of hypoeutectoidal Cu–Al–Ni shape memory alloys. J Alloys Compd 2009;470. https://doi.org/10.1016/j.jallcom.2008.03.009.

[58] Karaduman O, Canbay CA. Investigation of CuAlNi Shape Memory Alloy Doped with Graphene. Journal of Materials and Electronic Devices 2021;3:8–14.

[59] Saud SN, Hamzah E, Abubakar T, Bakhsheshi-Rad HR, Zamri M, Tanemura M. Effects of Mn Additions on the Structure, Mechanical Properties, and Corrosion Behavior of Cu-Al-Ni Shape Memory Alloys. J Mater Eng Perform 2014;23:3620–9. https://doi.org/10.1007/s11665-014-1134-1.